The Coronal Global Evolutionary Model (CGEM)

George H. Fisher, UC Berkeley, PI
Marc DeRosa, Lockheed Martin, Co-PI
Todd Hoeksema, Stanford University, Co-PI
and the CGEM Team

This project was selected under the 2011 Joint NASA/NSF opportunity for developing space-weather models. Funding started mid-2013.

Prior funding from NASA LWS-TRT, the NASA Heliophysics Theory Program, NSF AGS core research grants, and NASA funding for the SDO/HMI magnetic team at Stanford made this project possible.

What is the CGEM project?

The primary components of the CGEM project are:

1. Implement enhanced processing of SDO/HMI vector and full-disk line-of-sight magnetogram sequences and HMI Doppler measurement data and make these available to the Solar Physics and Space Weather communities
2. Use these data to compute electric fields at the photosphere, on both active-region and global scales
3. Use the time sequence of photospheric magnetic field and electric field maps to drive a time-dependent, non-potential model based on magnetofriction for the magnetic field in the coronal volume, both in active regions and globally. This will be done in spherical geometry, in either wedge-like configurations for active regions, or for the global Sun.
4. For unstable configurations found with the magnetofrictional model, perform follow-up studies using MHD models to provide more realistic dynamics for erupting magnetic structures

Why do CGEM?

- Solar-driven space weather events such as eruptive flares/CMEs are driven by the release of free magnetic energy that is stored in the low corona.
- Current data-driven space-weather coronal magnetic field models, based on potential fields, are unable to describe the buildup of free magnetic energy in the low corona.
- A prognostic, physics-based model of the solar magnetic field is possible by using time sequences of vector magnetic field observations

Why do CGEM now?

- The launch of SDO/HMI makes the data necessary to construct better coronal models regularly available
- Recent theoretical developments make it possible to derive electric fields from HMI data sequences using Faraday's law and Doppler data
- Recent computational methods for evolving the coronal magnetic field using a magneto-frictional model make it practical to evolve the coronal magnetic field on spatial and temporal scales that are useful
- We have demonstrated that an existing, Cartesian version of the model (the "CGEM Cartesian Prototype Model") is a viable model that can be run routinely on active region scales for periods of several days

Who is the CGEM team?

- UC Berkeley: George Fisher, Bill Abbett, Dave Bercik, Maria Kazachenko, Ben Lynch, Brian Welsch, …
- Lockheed-Martin Space Astrophysics Laboratory: Marc DeRosa, Mark Cheung, …
- Stanford University: Todd Hoeksema, Alberto Sainz Dalda, Keiji Hayashi, Yang Liu, Aimee Norton, Phil Scherrer, Xudong Sun, …

CGEM Project Responsibilties:
Berkeley: Overall direction of the project, Electric field software, electric field validation, project software management
Stanford: Enhancements to pipeline products, specialized vector magnetogram and dopplergram data reduction, new capabilities at JSOC
Lockheed: Development, validation, and implementation of the magnetofrictional model, flux transport model

Illustration of the HMI magnetic data
AR 11158 Feb. 12-16 2011 (Keiji Hayashi)

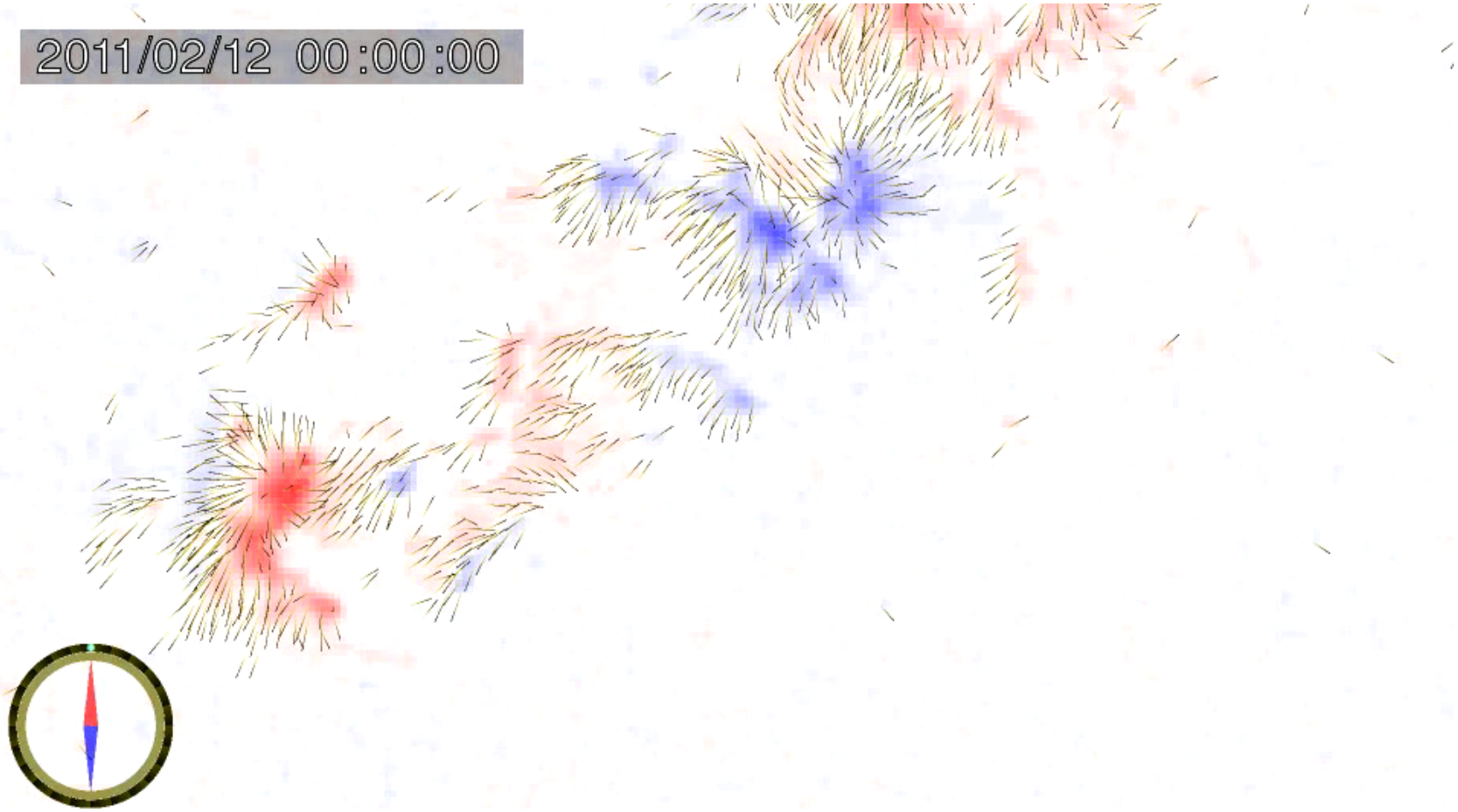

Goal of the CGEM project

Our primary goal is to expand our Cartesian proof-of-concept model into a community-wide coronal modeling tool, to cover the corona in spherical domains on (i) active region scales with high resolution, and (ii) a lower-resolution but fully global setting.

The results of this model will be used for both scientific studies, and tests of a physics-based prognostic model for space-weather purposes.

To achieve this goal, a number of CGEM deliverables were identified:

- D1: Develop a local spherical wedge and a global spherical magneto-frictional model
- D2: Develop or adopt a global flux transport model outside of SHARP regions to augment the vector magnetogram data within SHARP regions
- D3: Develop spherical wedge electric field solutions (from HMI data) inside of SHARP regions, and develop a global spherical solar electric field treatment driven by flux transport models
- D4: Incorporate new data products into the HMI pipeline to automatically generate Lorentz forces, electric field, Poynting flux and helicity flux outputs
- D5: Develop a simplified MHD model to follow unstable active region configurations found from MF simulations
- D6: Develop and refine global MHD solutions to connect the MF model with global heliospheric models
- Provide the JSOC and CCMC with working models of CGEM for community research and space-weather related applications

Progress on CGEM Deliverables during year one:

- D1: Cartesian Prototype MF model works well; a spherical version has been written and is now being tested
- D2: LMSAL Flux transport model is being converted from a "magneto-chemistry" technique to a grid-based model for compatibility with electric field inversions and MF model
- D3: Cartesian Electric Field code is stable and robust; a simple global spherical code has been written and has undergone some testing.
- D4: HMI Advanced data products – Horizontal and vertical Lorentz force maps now computed for all SHARPS observed by HMI, this dataset is now on JSOC. Other data products still under development.
- D5: RADMHD2S now runs on spherical wedge geometry; is being tested
- D6: Global MHD model, driven by global data from HMI, has been ported into the JSOC, and could probably be incorporated by CCMC anytime

Illustration of our Cartesian prototype MF model of the corona driven by B, E on photospheric boundary in AR11158:

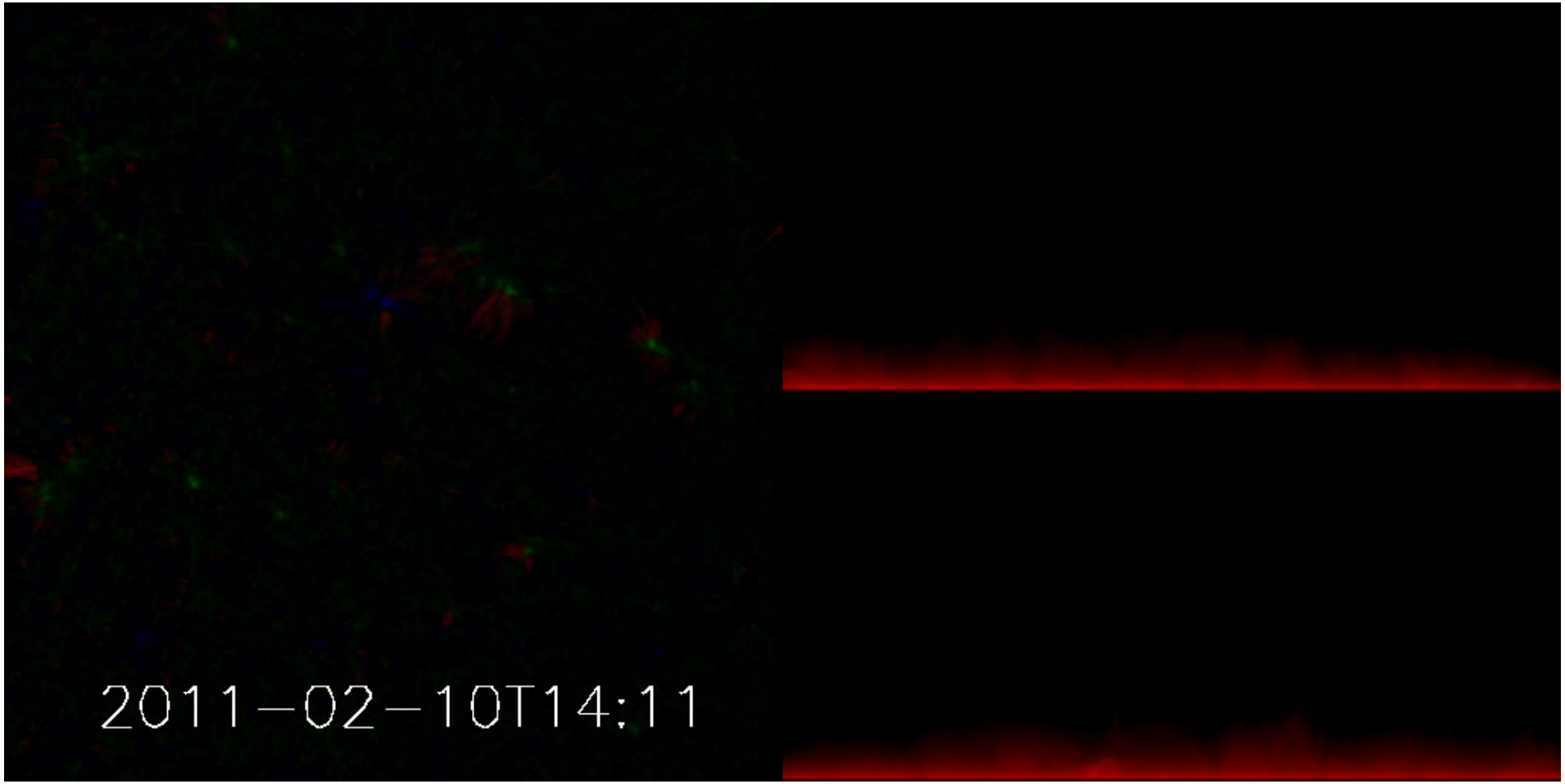

Magneto-frictional (MF) model of Cheung & DeRosa showing coronal evolution driven by magnetic fields from HMI, and electric fields derived by UCB from the Doppler and magnetic field measurements

Focusing on the time leading up to the X2.2 flare and shortly thereafter…

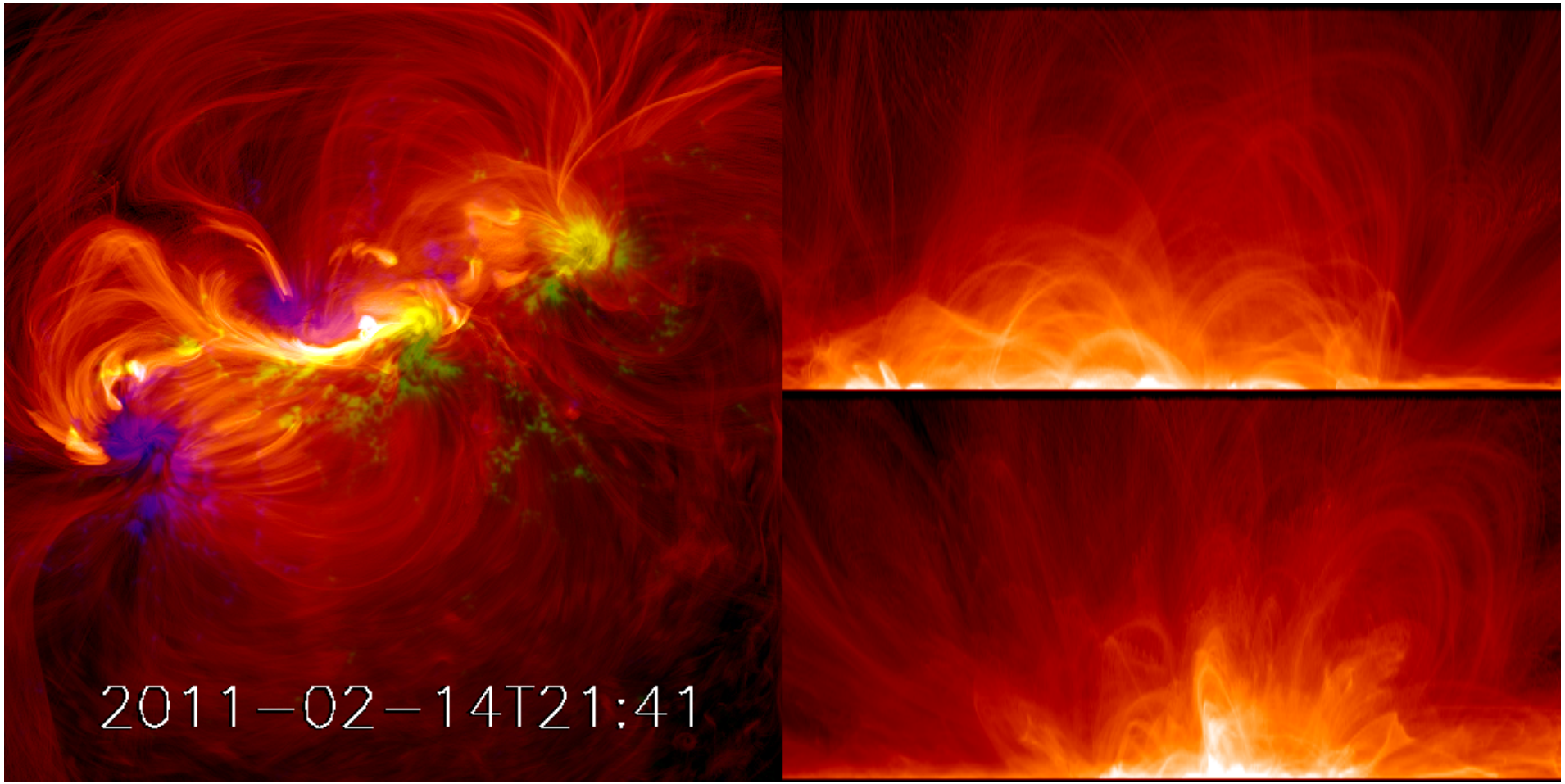

Highlights of the calculation just shown:

- HMI data of desired spatial, temporal (6+ days) window for AR 11158 (HMI Active Region Patch, or HARP) was extracted (Stanford)
- Corrections for 180-degree ambiguity errors, plus absolute scale Doppler shift corrections were applied, and were interpolated to a Cartesian grid (UCB, Stanford)
- Electric Fields were computed for the field-of-view (FOV) and 6-day time window, using observed magnetic field evolution and Doppler shifts (UCB)
- A magneto-frictional model was run for a Cartesian volume overlying the FOV for the desired time window (LMSAL)
- Since the CGEM proposal was submitted in March 2012, we've run through this procedure 4 more times, improving the data reduction procedure, the electric field calculations, and improving the numerical methods used in the magnetofrictional model.

Additional Processing of HMI of vector magnetogram and Doppler data

- The CGEM project requires that the 180 degree ambiguity resolution be done in such a way that the magnetic fields evolve physically in time
- The electric field determination (discussed later) requires calibration of Doppler shifts to ensure that the electric field near polarity inversion lines (PILs) is physically related to observed magnetic field evolution

Correcting the 180 degree ambiguity resolution

The left two columns show evolution in time (moving downward) of the transverse magnetic field azimuth for a subset of the AR 11158 data, and its change from the previous time, respectively, before the correction to the ambiguity resolution was applied. The right two columns illustrate the same two quantities, after our corrections have been applied. The spurious changes in ambiguity resolution show up in the 2nd column's difference images as dark blobs.

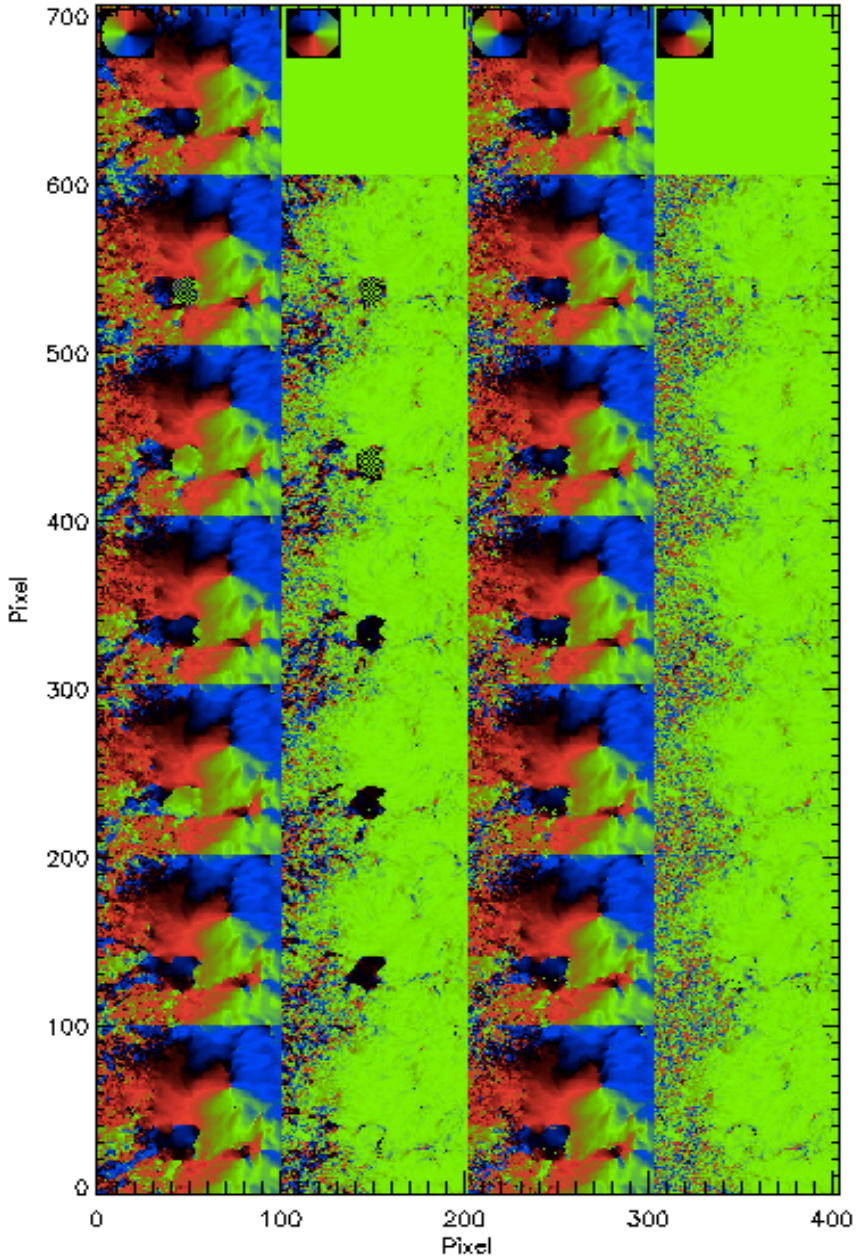

Absolute calibration of Doppler shifts

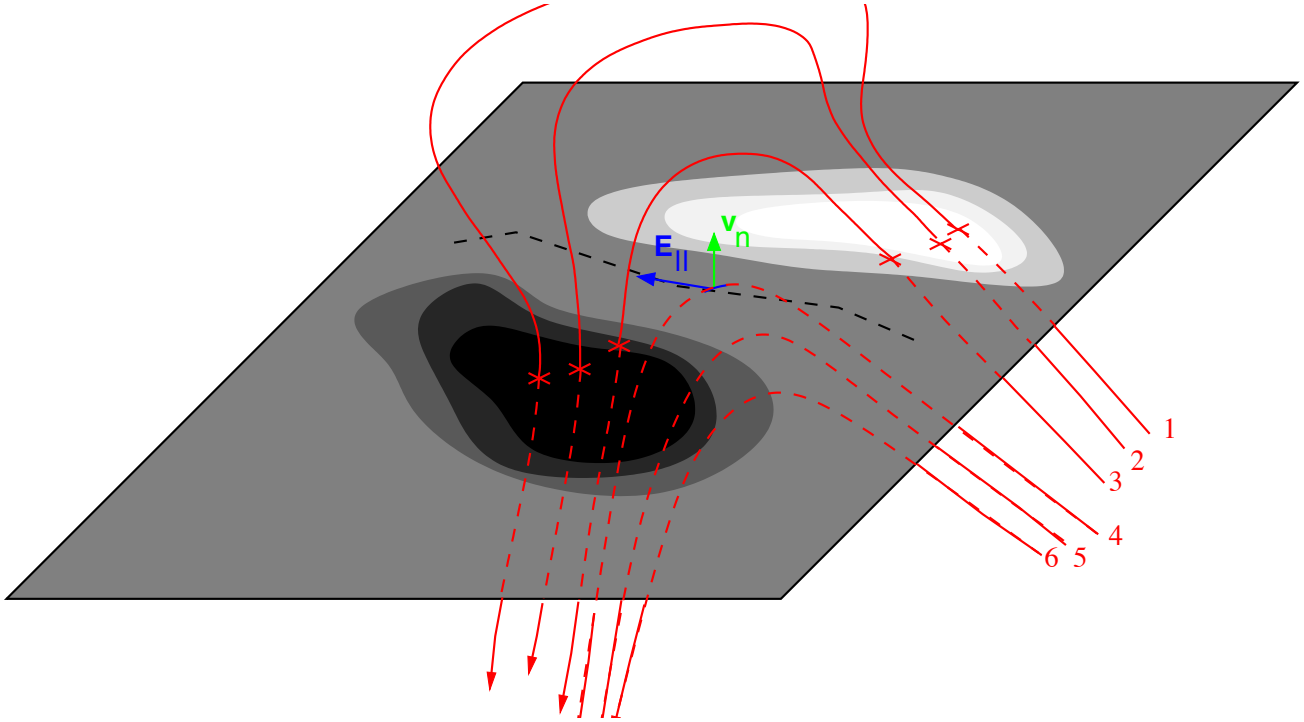

Doppler shifts as measured by HMI are biased by the convective blue-shift, resulting in an apparent red-shift of locations in which the vertical velocity should be zero. Welsch, Fisher, & Sun (2013) have developed a method of correcting for this bias, by insisting on consistency with Faraday's law for PILs near disk center.

Observed magnetic and Doppler evolution of AR 11158:

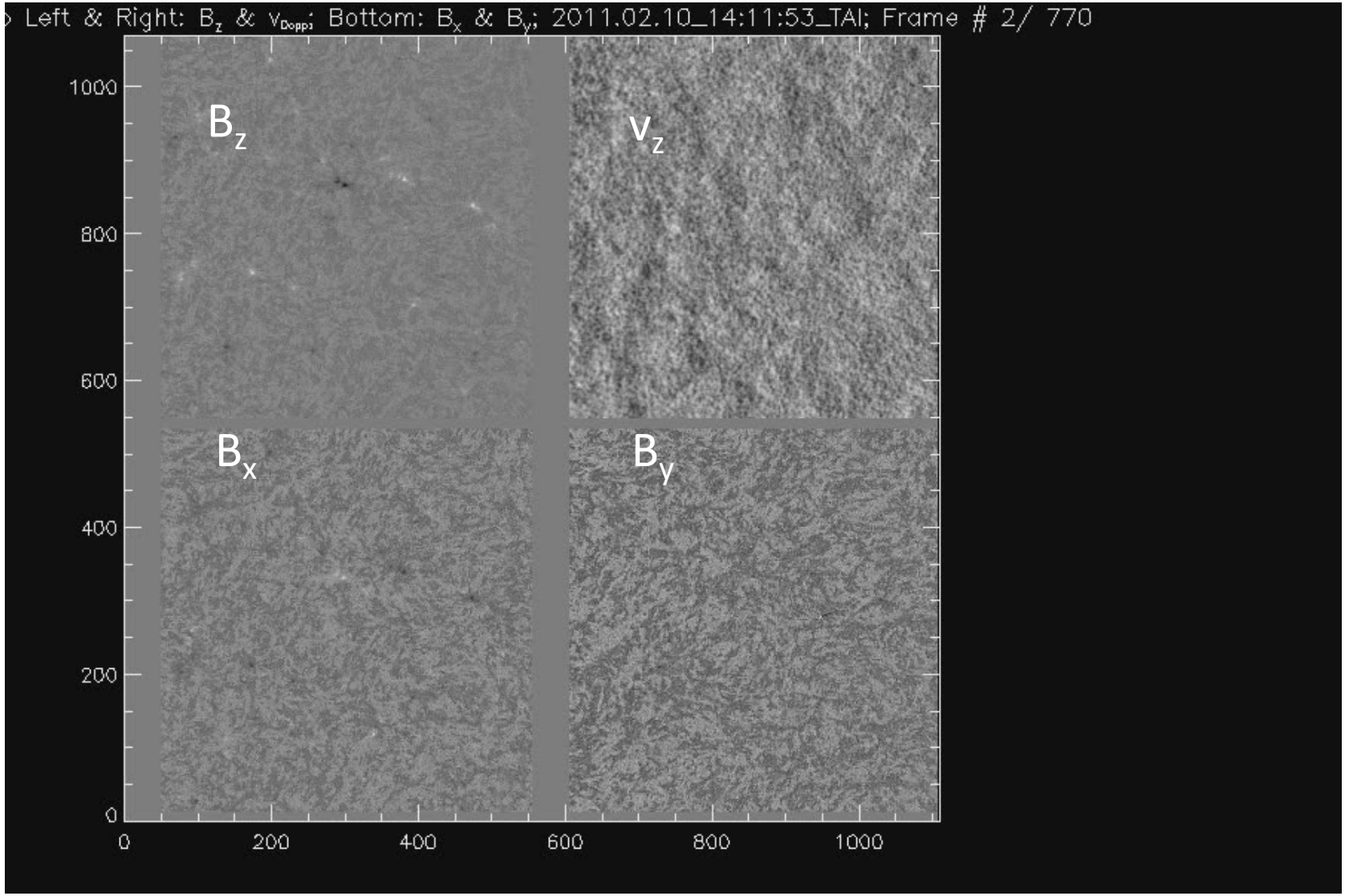

Comparison of uncorrected and corrected doppler shifts at PILs

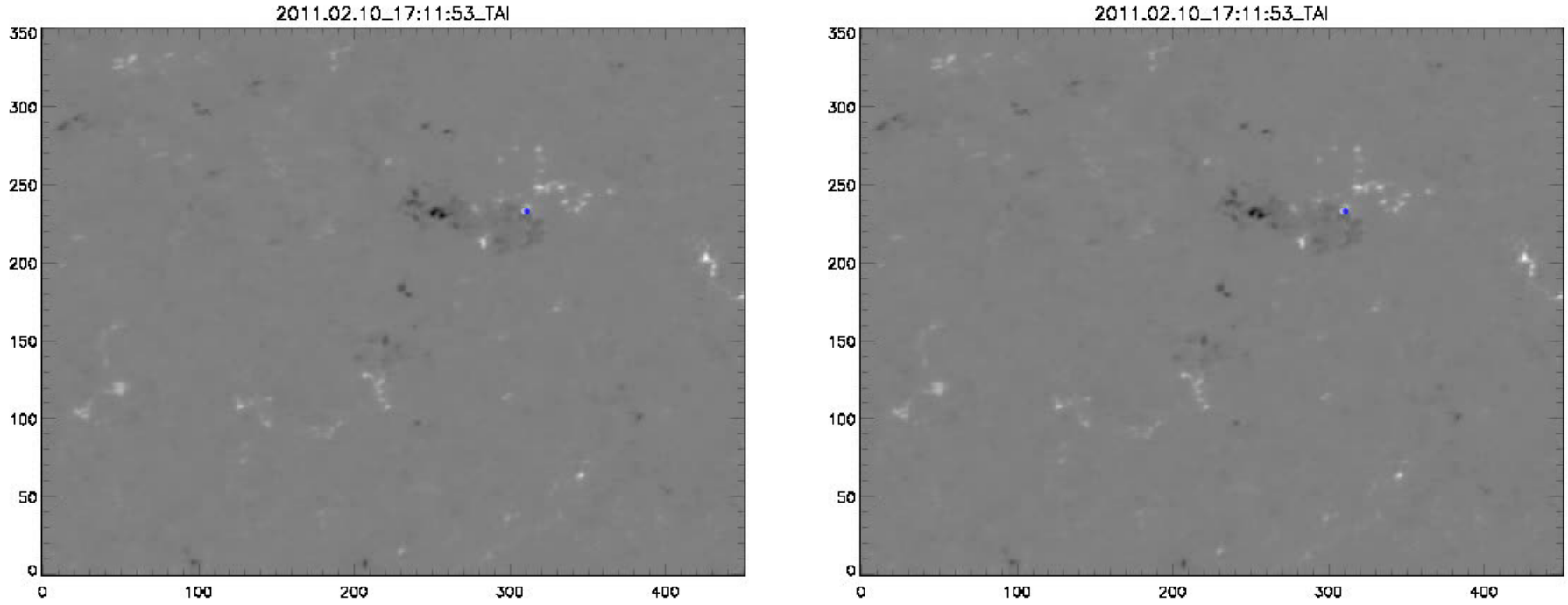

Left panel shows doppler shifts at polarity inversion lines without correction, right panel shows doppler shifts after correction has been applied.

Electric Field inversions from magnetic and Doppler data

Traditionally, the evolution of the magnetic field at the photosphere has been described in terms of a velocity field, motivated by the ideal MHD approximation, in which $cE = -v \times B$. Methods such as local-correlation tracking were used to find v. We have recently found it more useful to determine the electric field E itself, appealing to the ideal MHD approximation only when necessary. This change in paradigm is useful because (1) Faraday's law is true regardless of what causes the electric field, and (2) determining the velocity-field in weak-field regions is an ill-posed problem.

Details of electric field inversion technique, using vector magnetogram and Dopplergram sequences, can be found in Kazachenko et al (2014, ApJ in prep), Fisher et al (2012, Sol. Phys. 277, 153), and Fisher et al (2010, ApJ 715, 242).

How we determine electric fields: (1) Contributions from Faraday's Law

$$\dot{\mathbf{B}} = -\nabla \times c\mathbf{E}$$

$$\dot{\mathbf{B}} = (\dot{B}_x, \dot{B}_y, \dot{B}_z) = \underbrace{\nabla \times \nabla \times \dot{\beta}\hat{\mathbf{z}}}_{poloidal} + \underbrace{\nabla \times \dot{J}\hat{\mathbf{z}}}_{toroidal} = \underbrace{\nabla_h \left(\frac{\partial \dot{\beta}}{\partial z} \right) + \nabla_h \times \dot{J}\hat{\mathbf{z}}}_{horizontal} - \underbrace{\nabla_h^2 \dot{\beta}\hat{\mathbf{z}}}_{vertical}$$

$$\nabla \times c\mathbf{E} = -\nabla_h \left(\frac{\partial \dot{\beta}}{\partial z} \right) - \nabla_h \times \dot{J}\hat{\mathbf{z}} + \nabla_h^2 \dot{\beta}\hat{\mathbf{z}}$$

$$c\mathbf{E} = -\left(\nabla_h \times \dot{\beta}\hat{\mathbf{z}} + \dot{J}\hat{\mathbf{z}} \right) - \nabla\psi = c\mathbf{E}_I - \nabla\psi$$

The Poloidal and Toroidal potentials are determined by these three two-dimensional Poisson equations

$$\nabla_h^2 \dot{\beta} = -\dot{\mathrm{B}}_z \quad ;$$

$$\nabla_h^2 \dot{J} = -\frac{4\pi \dot{J}_z}{c} = -\hat{\mathbf{z}} \cdot (\nabla_h \times \dot{\mathbf{B}}_h) \quad ;$$

$$\nabla_h^2 \left(\frac{\partial \dot{\beta}}{\partial z} \right) = \nabla_h \cdot \dot{\mathbf{B}}_h$$

We refer to the electric field found from this formalism as the "Poloidal-Toroidal Decomposition" (or PTD) electric field

How we determine electric fields: (2) from Doppler shifts and transverse fields

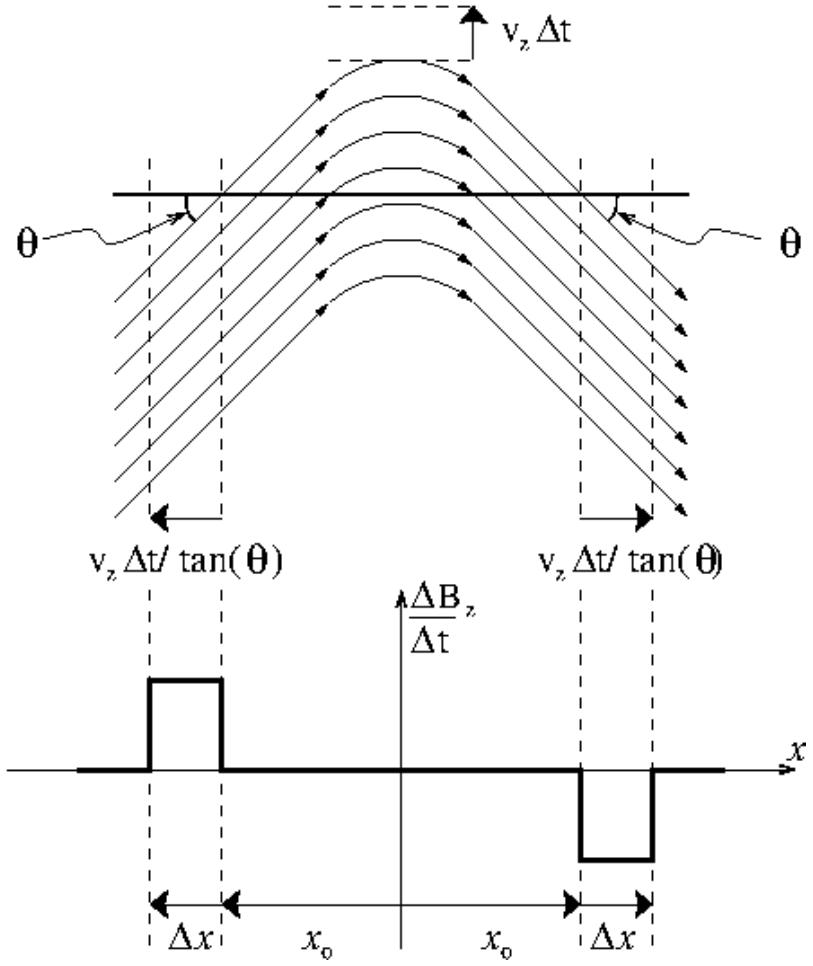

We have argued that there must also be substantial electric fields from the gradient of a potential function that can be related to flux emergence… (Fisher, Welsch & Abbett, Sol. Phys. 277, 153). Near a Polarity inversion line,

$$c\mathbf{E} = -\mathrm{v}_z \hat{z} \times \mathbf{B}_\mathbf{h}$$

We find a potential function that gives the correct **E** near PILs.

Electric field inversions: validation with MHD simulation

Top 3 panels show the 3 components of E from our ANMHD test simulation of a magnetic bipole emerging in turbulent convection. The middle 3 panels show the same quantities, where the inverted electric field incorporates the PTD contributions, the Doppler shifts near PILs, and smaller corrections for non-inductive correlation tracking flows and an additional potential added to enforce the condition $\mathbf{E} \cdot \mathbf{B}=0$. Bottom 3 panels show scatter plots of inverted versus actual electric field components.

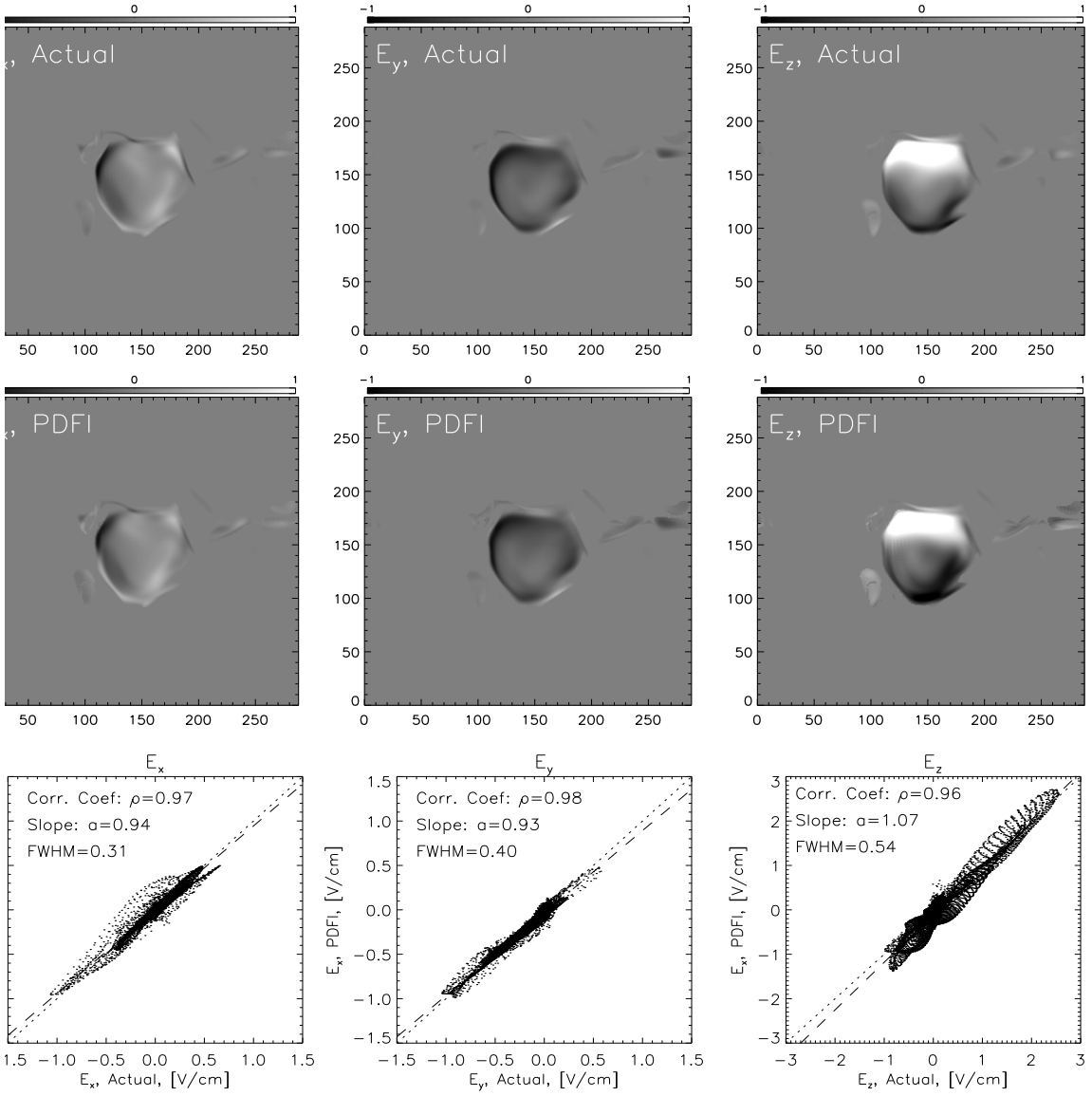

Poynting flux validation:

$$S_z = \frac{c}{4\pi}(E_x B_y - E_y B_x)$$

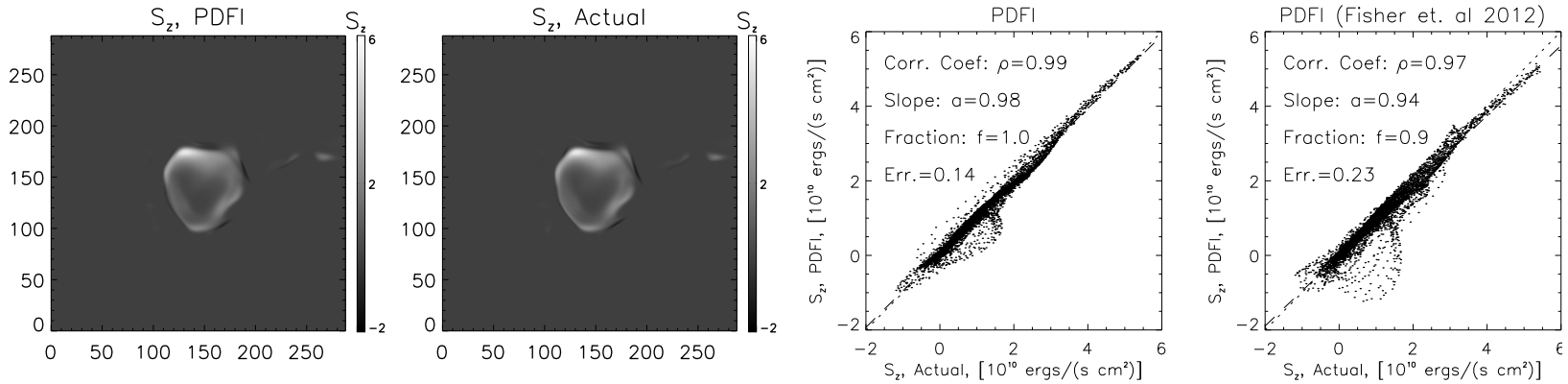

Qualitative and quantitative comparisons show good recovery of the simulation's **E**-field and vertical Poynting flux S_z.

Get Poynting flux and flux of free magnetic energy for AR 11158:

First, do poloidal-toroidal composition of **B** itself:

$$\mathbf{B} = (B_x, B_y, B_z) = \underbrace{\nabla \times \nabla \times \beta \hat{z}}_{poloidal} + \underbrace{\nabla \times J\hat{z}}_{toroidal} = \underbrace{\nabla_h \left(\frac{\partial \beta}{\partial z} \right) + \nabla_h \times J\hat{z}}_{horizontal} - \underbrace{\nabla_h^2 \beta \hat{z}}_{vertical}$$

This then allows you to break apart the Poynting flux into two parts:

$$S_z = \frac{c}{4\pi}(E_x B_y - E_y B_x) = \frac{c}{4\pi}\left[E_x \left(\frac{\partial J}{\partial x} - \frac{\partial}{\partial y}\frac{\partial \beta}{\partial z} \right) - E_y \left(-\frac{\partial J}{\partial y} - \frac{\partial}{\partial x}\frac{\partial \beta}{\partial z} \right) \right] =$$

$$\underbrace{\frac{c}{4\pi}\left(E_x \frac{\partial J}{\partial x} + E_y \frac{\partial J}{\partial y} \right)}_{S_{zfree}} + \underbrace{\frac{c}{4\pi}\left(-E_x \frac{\partial}{\partial y}\frac{\partial \beta}{\partial z} + E_y \frac{\partial}{\partial x}\frac{\partial \beta}{\partial z} \right)}_{S_{pot}}$$

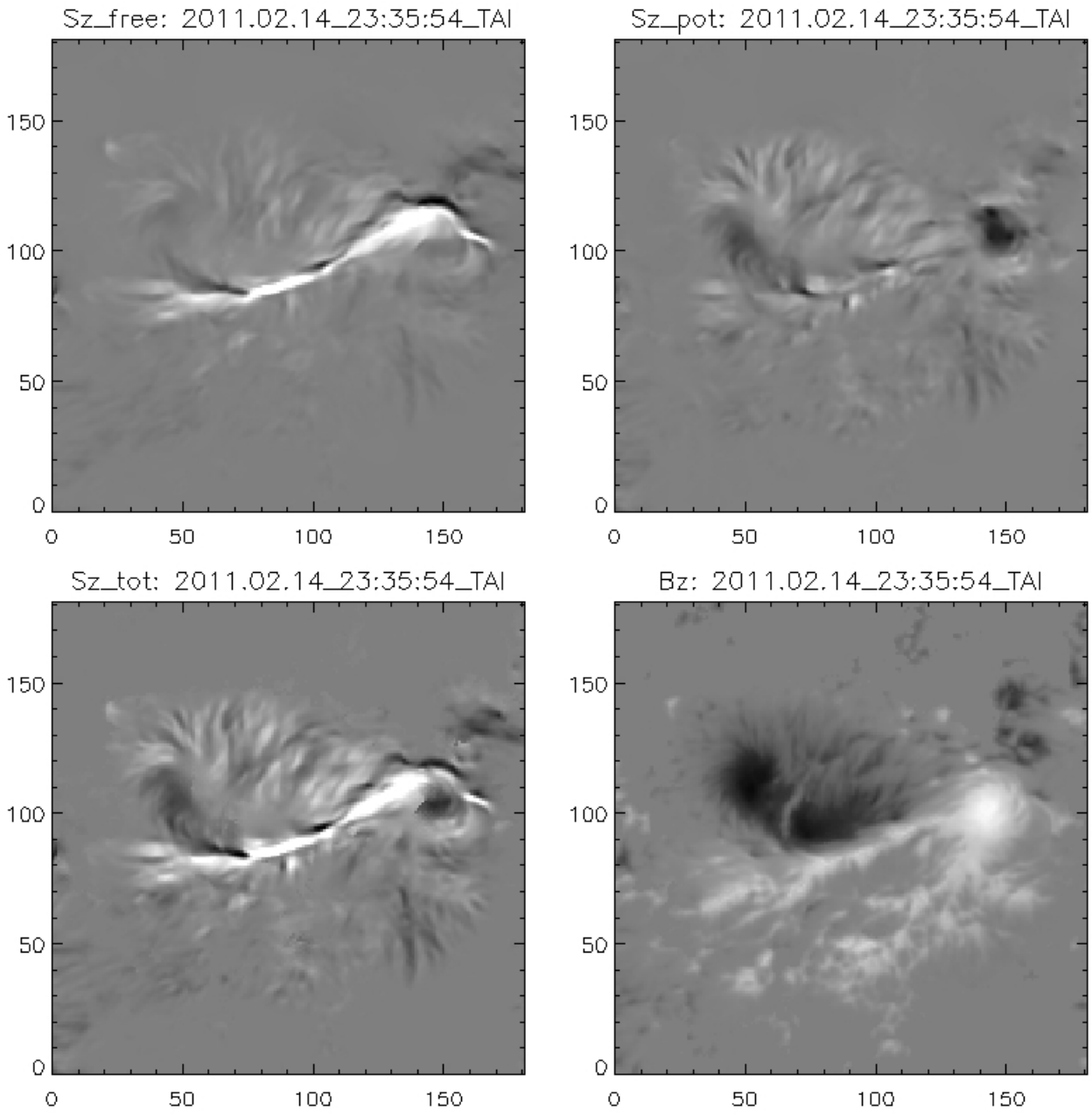

Evolution of Sz components around flare time: *Two top panels:* Two parts of the vertical Poynting flux: the flux of free magnetic energy and the flux of potential-field energy. *Bottom Left:* The sum of the two parts, i.e. the total vertical Poynting flux; *Bottom Right:* Vertical magnetic field Bz observed by HMI. White (black) shows positive (negative) values. All plots are for time period from 23:35 UT Feb 14 to 05:35 UT Feb 15. The X2.2 flare peaks at 01:56 UT on Feb 15 2011.

Illustration of the use of HMI data to derive Electric Fields (to compute a vertical Poynting flux)

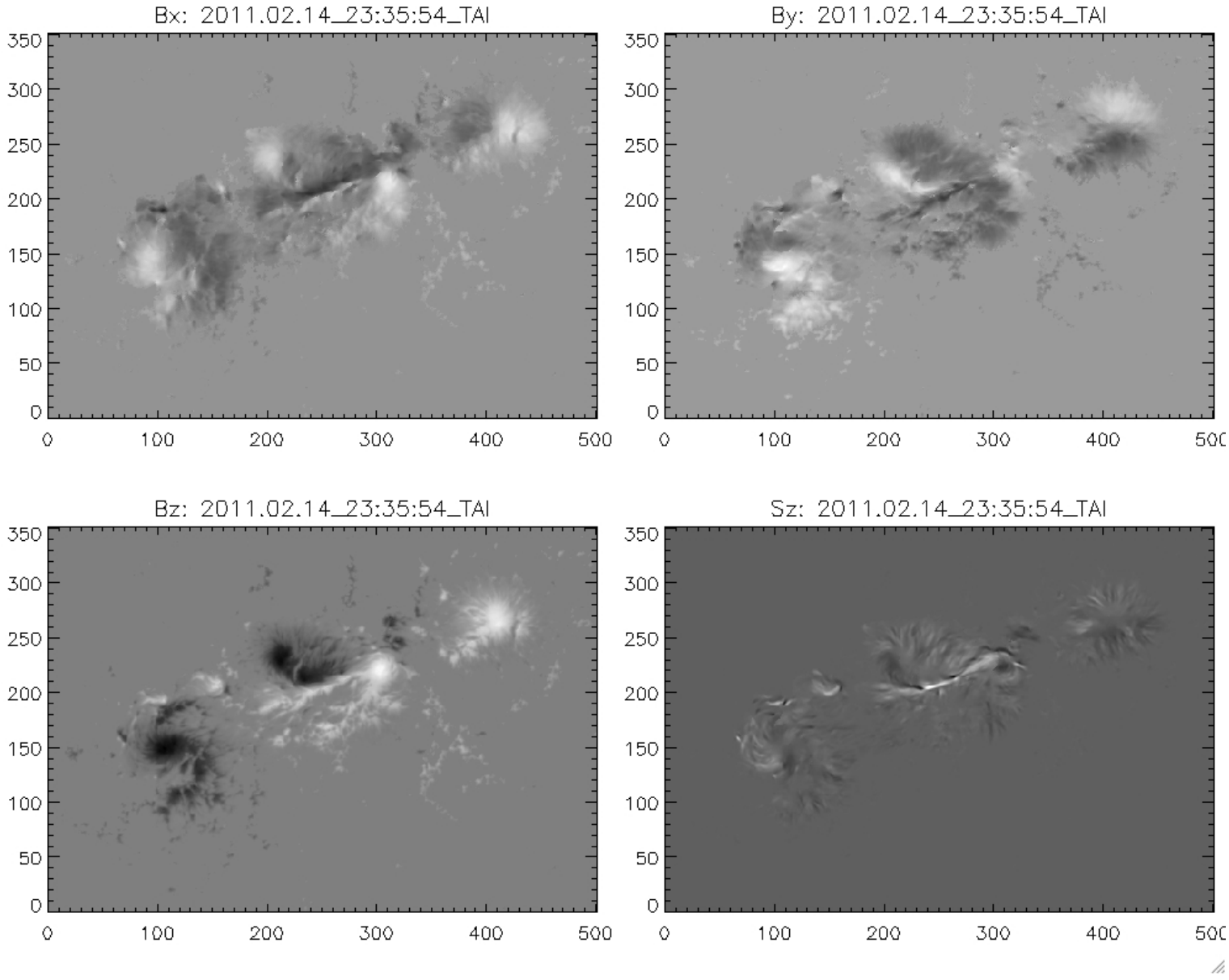

Magnetofriction

Balance the Lorentz force with a fictitious frictional force (Yang, Sturrock & Antiochos, 1986; Craig & Sneyd 1986)
Set the plasma velocity proportional to Lorentz force:

v= ν_0^{-1} $\boldsymbol{j}$x$\boldsymbol{B}$ where ν_0 is the frictional coefficient. Evolve the magnetic field according to the induction Equation.

The total magnetic energy in the volume monotonically decreases (if the net Poynting flux through boundaries is zero).

We use the temporal sequence of magnetograms and electric fields, and update the model forward in time

Magnetofriction (cont'd)

Van Ballegooijen, Priest & Mackay (2000)

- Evolve vector potential $\boldsymbol{A}$
- Plasma velocity proportional to Lorentz force: $\boldsymbol{v} = (\nu_0 B^2)^{-1} \boldsymbol{jxB}$

Yeates, Mackay & Van Ballegooijen (2008)

- Global magnetofrictional model of coronal field in response to observed changes in photospheric field, including
  - Differential rotation, meridional circulation
  - Flux dispersal and cancellation
  - Appearance of AR-scale, twisted bipoles
- Correctly reproduces filament chirality and location
- Memory of corona ~ 6 weeks to a few months

Nice review of global solar magnetofrictional models: Yeates (2014, Sol. Phys, 289, 631) also arxiv:1304.0609)

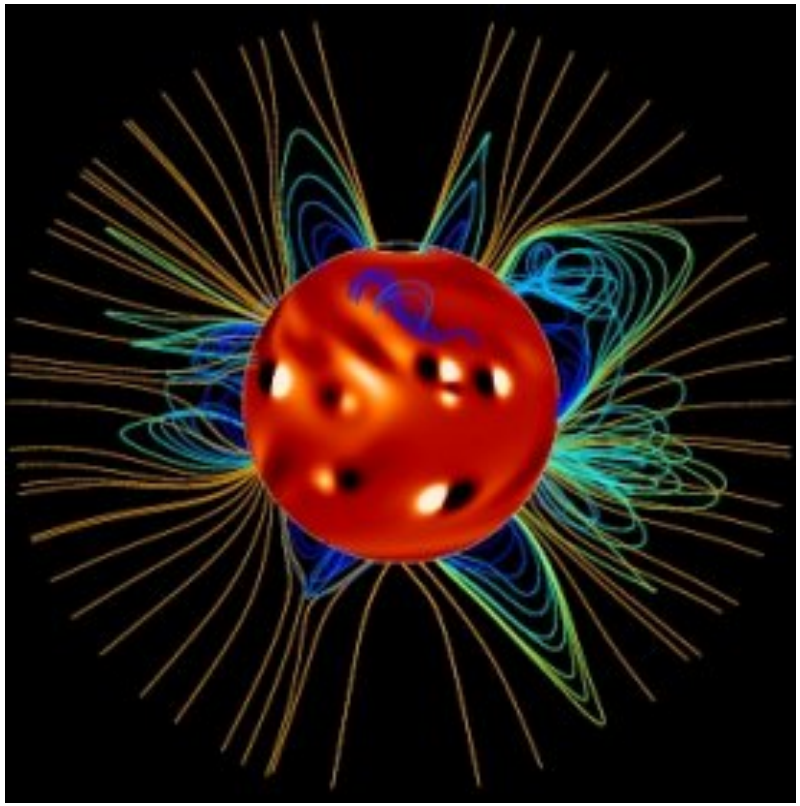

Yeates, Mackay & Van Ballegooijen 2008

Magnetofriction (cont'd)

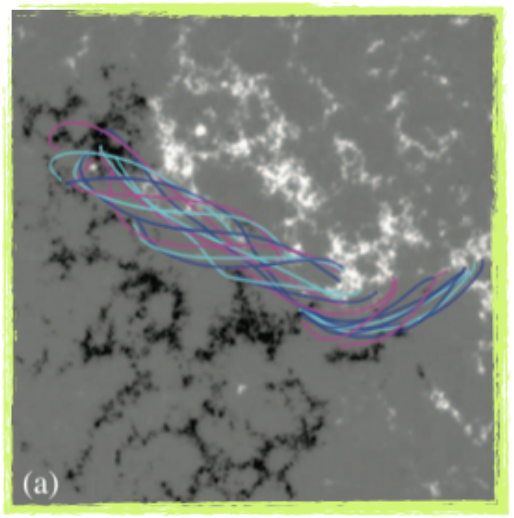

Modeling of filaments/prominences (van Ballegooijen 2004, van Ballegooijen 2007; Bobra, van Ballegooijen, DeLuca 2008; Su et al 2009) by inserting a flux rope into a potential field and relaxing using magnetofriction.

- Ejection of flux ropes (Yeates & Mackay 2009; Yeates et al 2010)

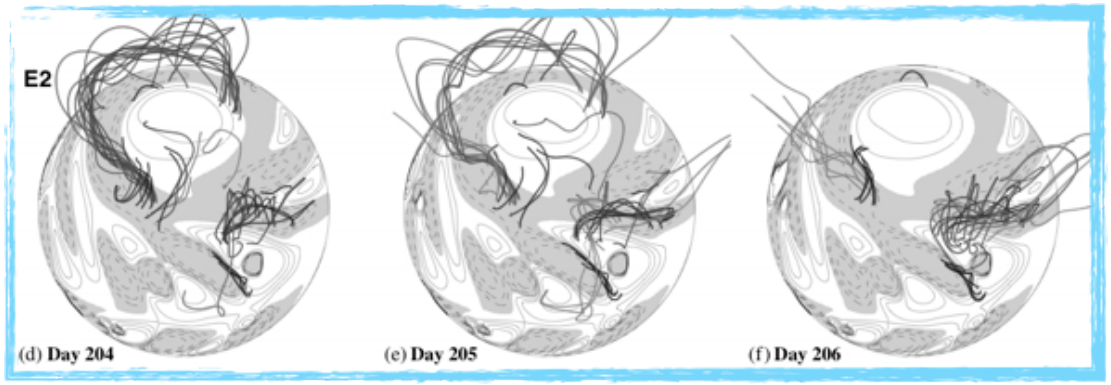

Numerical implementation

Is based on method described in Van Ballegooijen, Priest & Mackay (2000)

- Induction Equation for ***A***
- Staggered Cartesian grid
  - A_i, j_i at midpoint of cell edges along i-th direction
  - $\boldsymbol{B_i}$ at center of cell face with normal vector in i-th direction
- Spatial derivatives: 2nd order finite difference
- Magnetic diffusivity imposed to smooth current sheets at the grid-scale.
- Time integration: Explicit 2nd order
- MPI parallelized by domain decomposition
- See Cheung & DeRosa (2012) for details

$$\frac{\partial \vec{A}}{\partial t} = \vec{v} \times \vec{B} - \eta \vec{j}$$

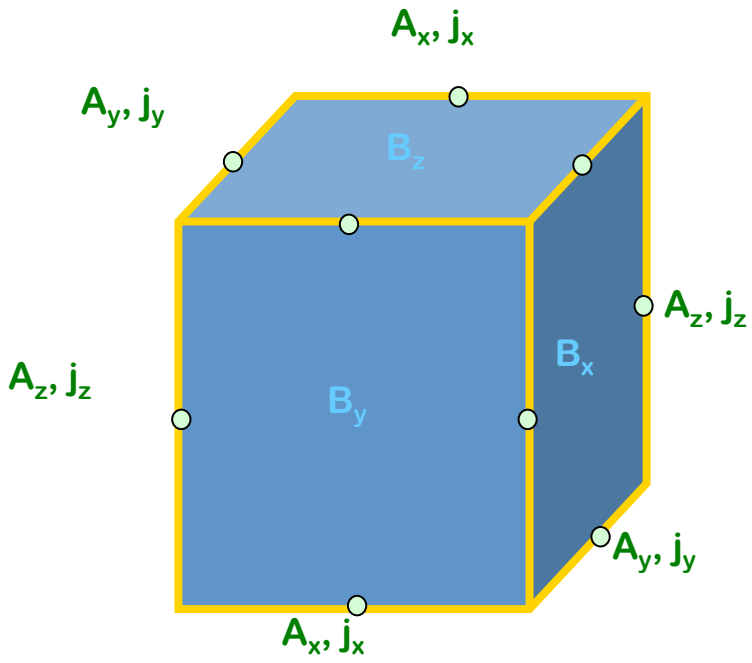

Initial and boundary conditions

- **Initial condition: Potential field extrapolation from magnetogram at t=0.**
- **Top and side boundaries**
  - **Field is assumed to be normal to boundary and velocities are continuous across boundary.**
- **Bottom boundary**
  - **Impose horizontal components of the electric field as time rates of change of A_x and A_y.**
  - **Assume $\nabla_h \cdot \underline{E_h}' = 0$ and use Fourier method to determine E_x' and E_y'. This is not a well-constrained problem. See Fisher et al (2010 and 2012) for details.**

Initial and boundary conditions

- **Bottom boundary**
  - **At each time step, determine the discrepancy between the simulated B_z^{sim} with the input B_z^{in}.**
  - **Let E_h' be the horizontal electric field that corrects this discrepancy.**
  - **Then $curl\{E_h'\} = \{B_z^{in} - B_z^{sim}\}/\Delta t$, where Δt is the time-step.**
  - **Assume $\nabla_h \bullet E_h' = 0$. Use Fourier method to determine E_x' and E_y'.**
  - **Use E_x' and E_y' to modify A_x and A_y at the bottom boundary. The updated A_x and A_y at the boundary has $B_z^{sim} = B_z^{out}$.**

3D Visualization

Orange $\propto L^{-1} \int j^2 \, dl$

Lavender $\propto L^{-1}(B/B_{base})(\int j^2 \, dl)$

Not much free energy

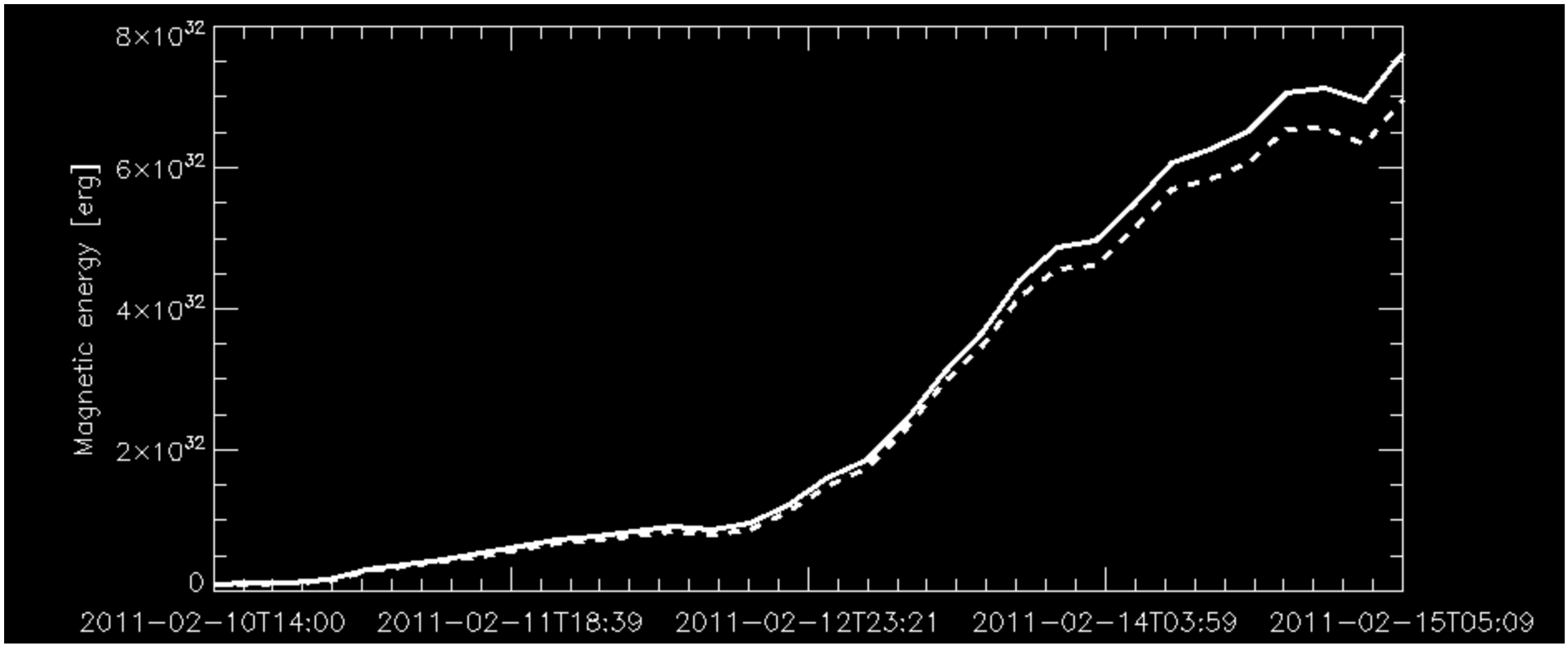

- At any point in time, the free energy is just a few % of the potential field energy.

Introduce twisting motion

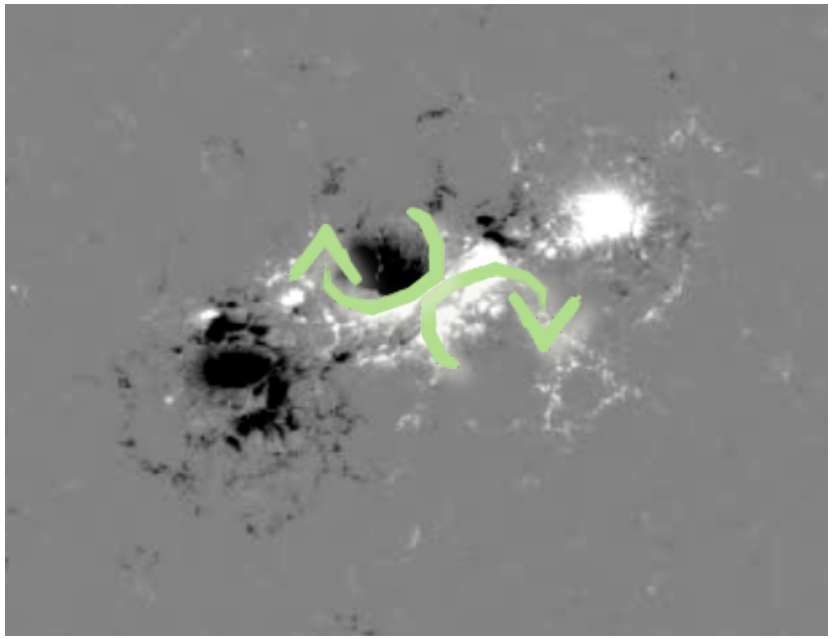

–Sunspots are known to rotate (Longcope & Welsch 2003; Brown et al 2003; Canou et al 2009, Brown et al 2011).

–Assume $\nabla_h \cdot \underline{E_h}' = \omega_z \underline{B_z}$, where ω_z is the vertical component of the vorticity of the footpoint motion.

–For simplicity, ω_z is chosen to have the same sense for both positive and negative polarities (see Fan 2009).

ω = 1/4 turn per day

Orange $\propto L^{-1}\int j^2\, dl$ Lavender $\propto L^{-1}(B/B_{base})(\int j^2\, dl)$

Recurrent Flux Rope Ejections

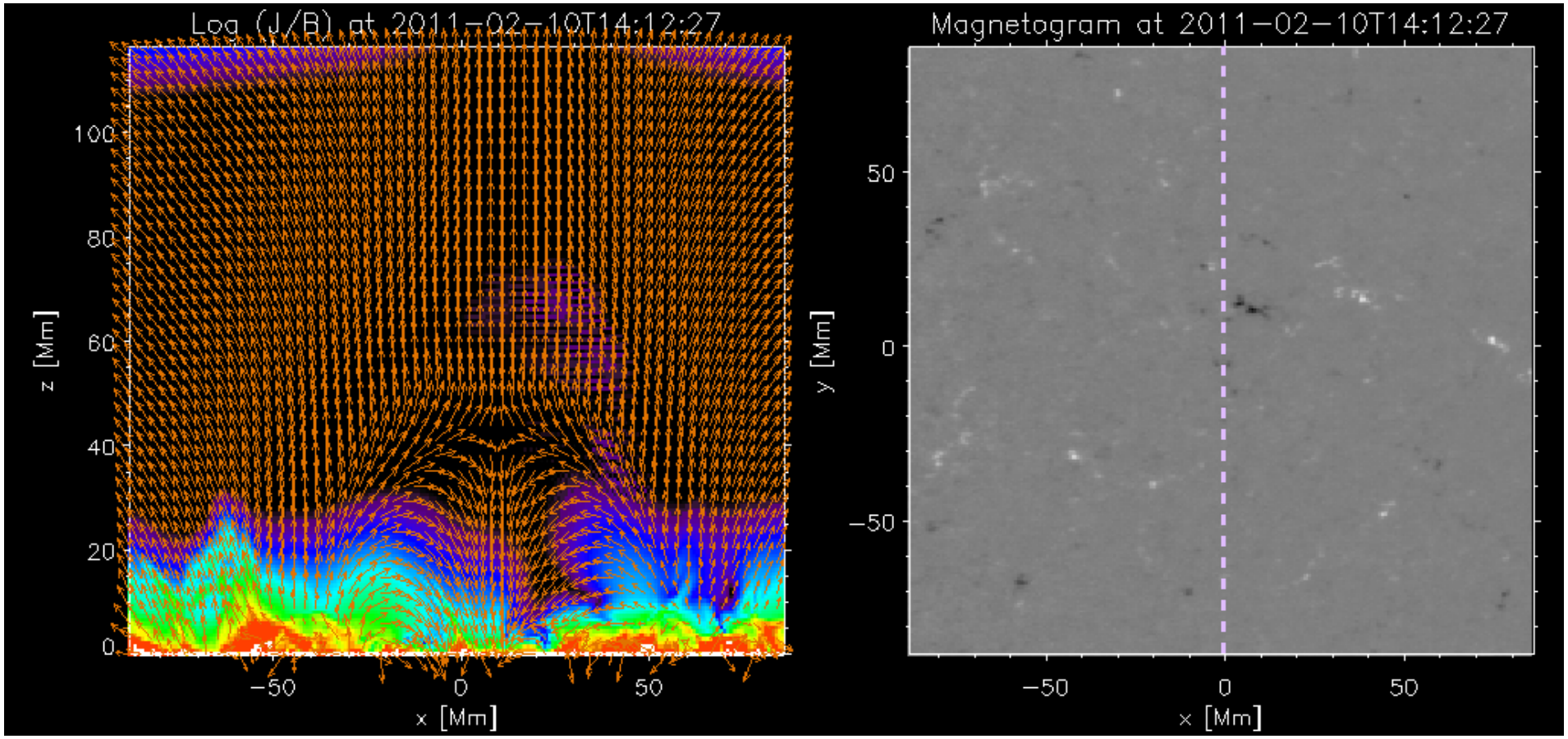

- Sheared field results in (multiple) flux-rope ejections (cf. Mikic & Linker 1994; Antiochos, DeVore & Klimchuk 1998; Manchester et al 2004).

Using E-fields retrieved from HMI magnetograms

- Use temporal sequences of vector magnetograms and Dopplergrams to constrain the photospheric electric field.
- Description of method: Fisher, Welsch & Abbett (2012).
- Application to SDO/HMI vector magnetograms: Kazachenko, Fisher, & Welsch (2013, in prep)
- Data-driven model using their E-field inversion results: next slide

Simulation driven using retrieved E-fields from Kazachenko et al. for AR 11158:

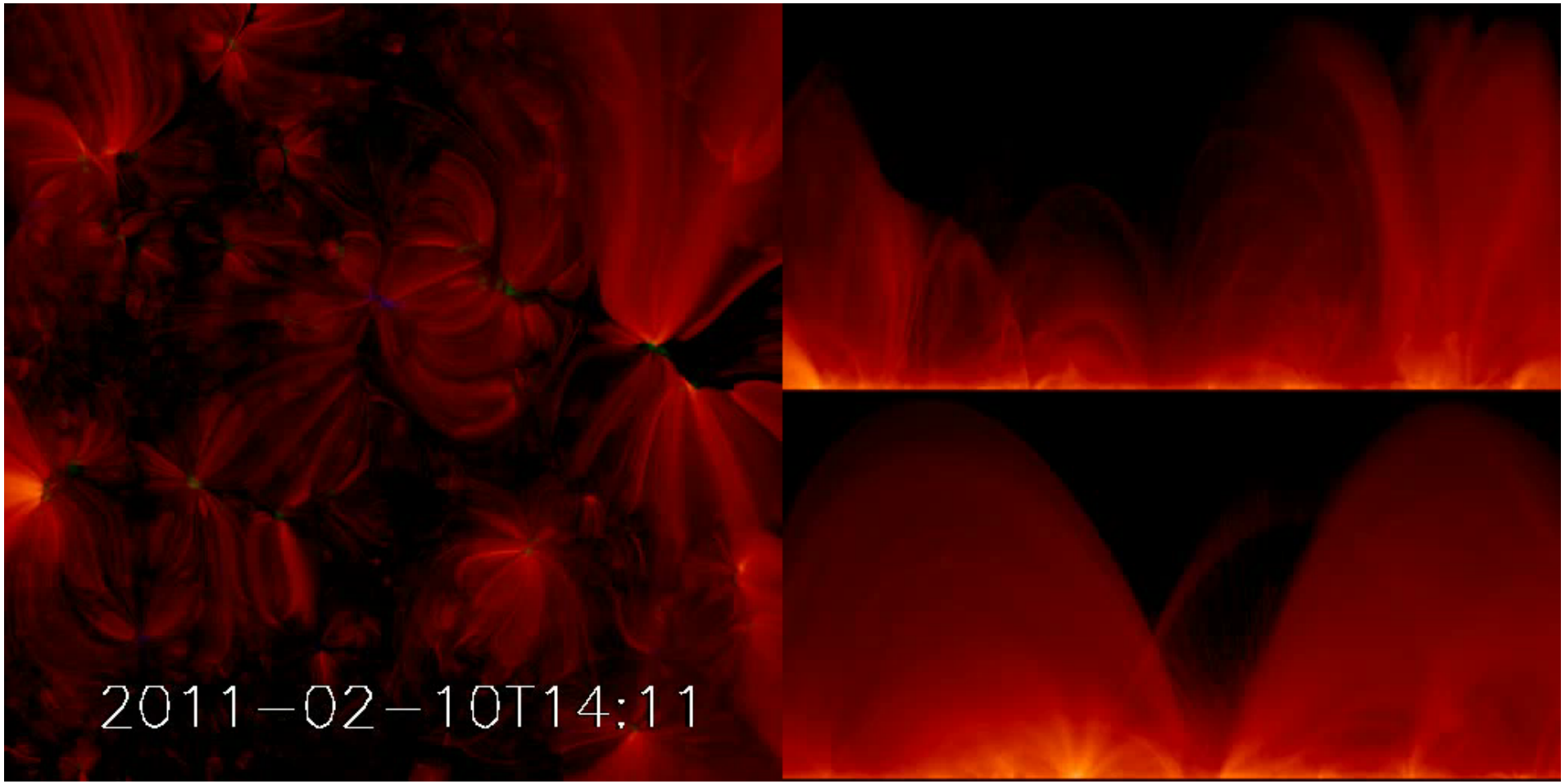

Color ~ log ($L^{-1}\int j^2\, dl$) integrated along line-of-sight

AR11158: Evolution of Free Magnetic Energy

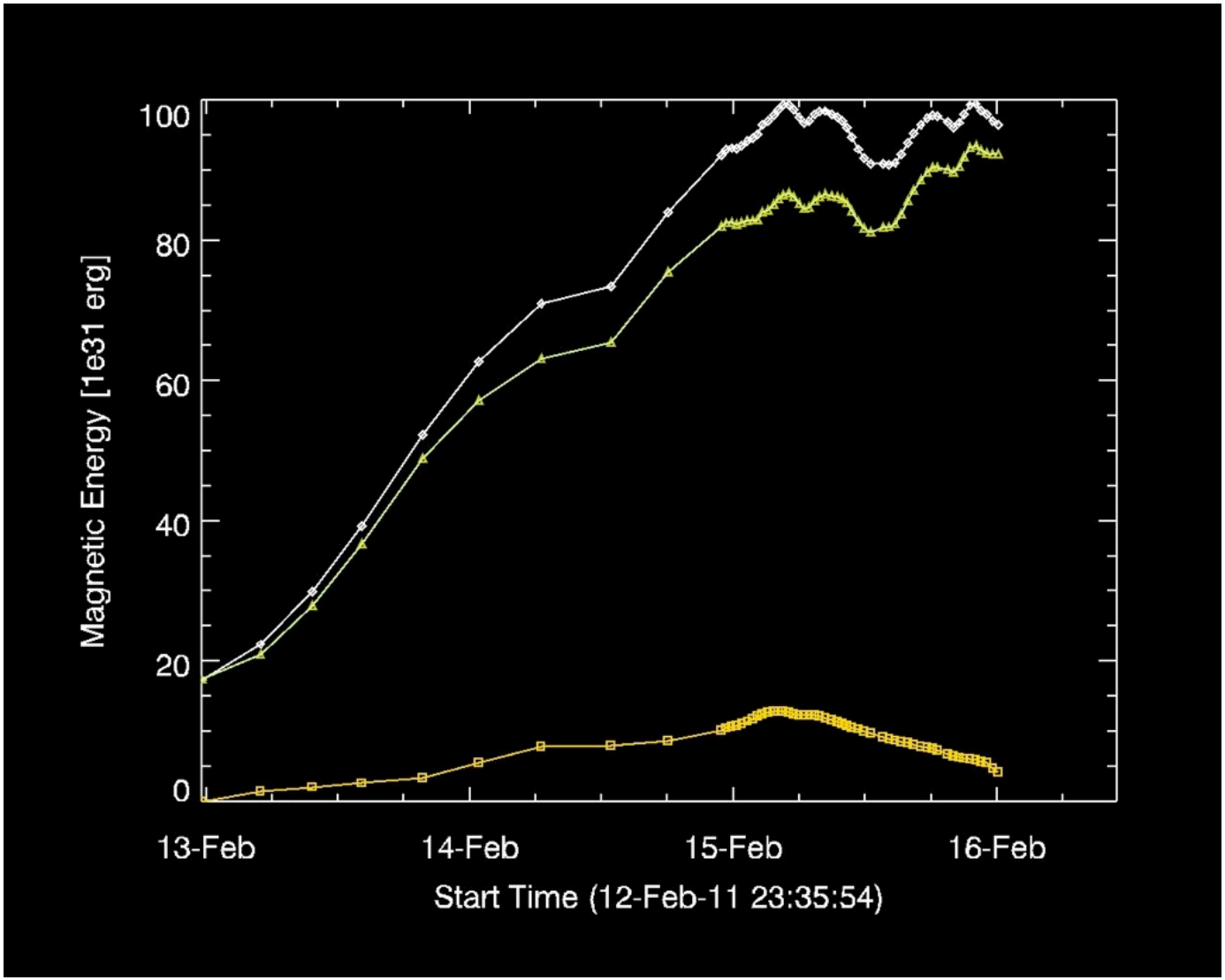

Helicity-Energy Relation

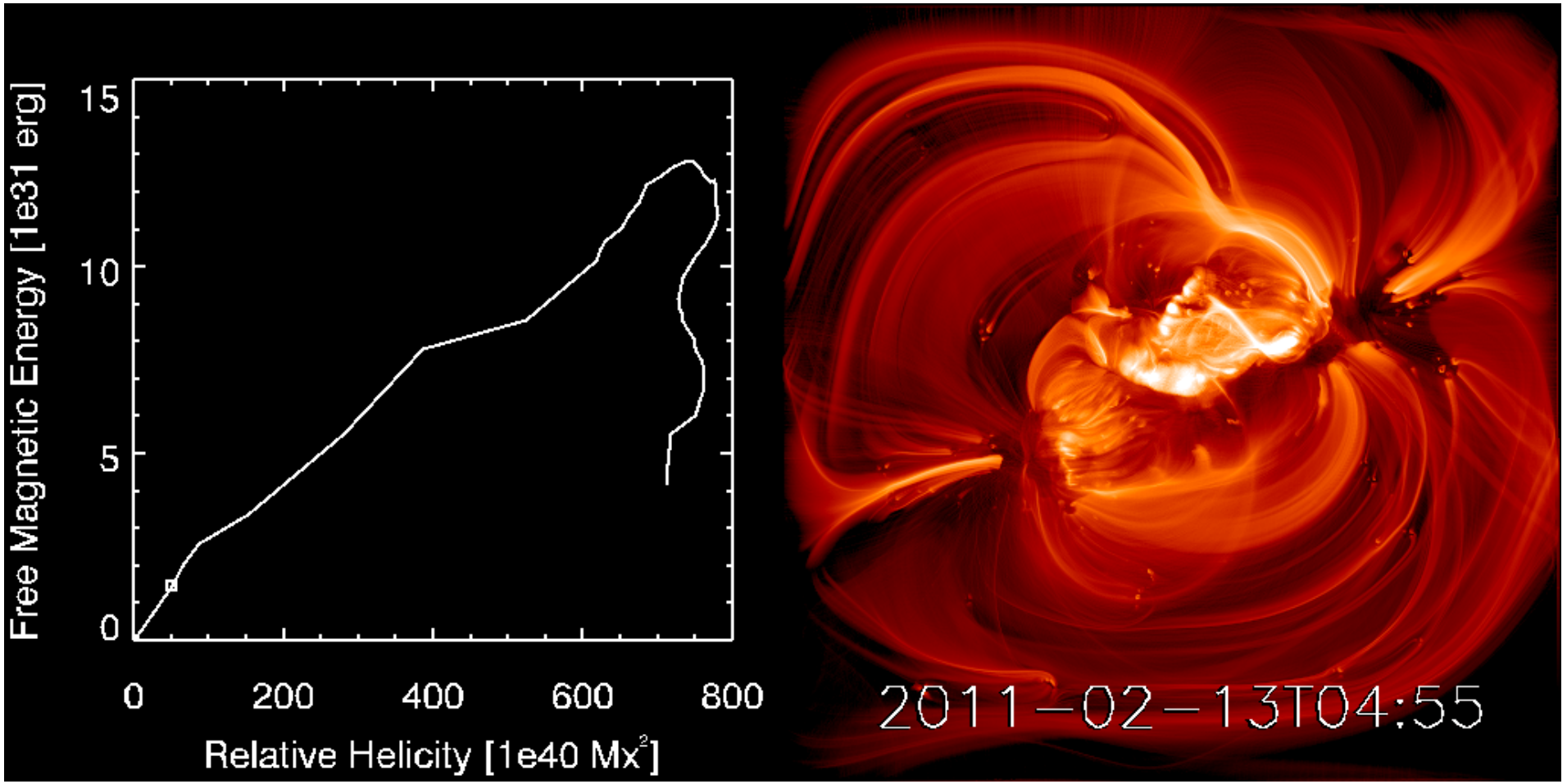

$H_{rel} = \int(\boldsymbol{A}+\boldsymbol{A_p}) \cdot (\boldsymbol{B}-\boldsymbol{B_p})dV$ (Finn & Antonsen 1985)

Summary of CGEM status

- We are currently preparing at least three publications describing our collaborative efforts for the Cartesian case
- The development of the spherical coordinate community-based model is underway
- We are eager to collaborate with the other strategic modeling efforts which could improve our inputs and make use of the output from our model
- We are all very excited about the project!

What is CGEM really?